

# The Microstructure of Ultrafine Eutectic Au-Sn Solder Joints on Cu

H.G. SONG,<sup>1</sup> J.W. MORRIS, Jr.,<sup>1</sup> and M.T. McCORMACK<sup>2</sup>

1.—University of California, Department of Materials Science and Engineering, Berkeley, CA 94720; and Lawrence Berkeley National Laboratory, Center for Advanced Materials.

2.—Fujitsu Computer Packaging Technologies, San Jose, CA 95134

The present work studies the microstructure and microstructural evolution of small volumes of nominally eutectic Au-Sn solder on Cu. The study includes solder bumps 140–145  $\mu\text{m}$  in diameter and 55–65  $\mu\text{m}$  tall deposited on Cu-plated Si, and solder joints 60  $\mu\text{m}$  in diameter and 25  $\mu\text{m}$  in height that join Cu-plated ceramic and polyimide substrates. The results show that the microstructure is strongly affected by the addition of Cu from the substrate during reflow, which produces a thick intermetallic layer along the interface. In the case of the joints, normal processing produces a coarse microstructure that includes only a few grains between thick intermetallic coatings. Aging at high temperature causes a further monotonic increase in Cu content, which alters the intermetallic structure at the interfaces and can lead to intermetallic bridging across the joint. Thermal fatigue tests suggest that cyclic deformation breaks up the intermetallic structure, increasing the rate of Cu addition to the joint, but refining the apparent grain size.

**Key words:** Au-Sn solder, ternary Au-Cu-Sn compounds, aging treatments

## INTRODUCTION

The miniaturization of microelectronic packages requires the use of increasingly dense arrays of interconnects with increasingly fine solder joints. The miniaturization of the solder joints raises two issues that need to be addressed to design reliable packaging.<sup>1</sup>

First, when the solder joint is very small the microstructural features that govern its mechanical behavior (such as the mean grain size) may be large with respect to the size of the joint. If the joint contains only a few grains it is not obvious if or how its mechanical behavior can be predicted from conventional mechanical tests, and there may be a considerable variation in behavior from joint to joint.

Second, when the thickness of the joint becomes small its composition can be changed significantly by diffusion from the substrates to which it is bonded. This is particularly likely when the substrate is Cu or Au, which diffuse fairly rapidly into most common solders.<sup>2,3</sup> The microstructure and properties of a small solder joint can be affected by minor changes in the details of processing, and may change further as the joint is strained and heated during service.

The present paper addresses a part of this problem by studying the microstructure and the evolution of microstructure in nominally eutectic Au-Sn solders on Cu. The solders were prepared as small bumps or joints with linear dimensions of 60–140  $\mu\text{m}$ , made by the commercial Z-MAJIC<sup>TM</sup> process.<sup>4</sup> We studied the microstructures in the as-solidified condition, and followed their development during aging. The results show that the initial microstructure can be quite coarse on the scale of the joint, and that both the microstructure and phase distribution can change significantly as the solder accumulates Cu from the substrates during aging. We did not attempt to determine the mechanical properties of the joints or the constituent phases in this work, though the need for such an investigation will become apparent.

## EXPERIMENTAL PROCEDURE

The two sets of samples used in this work are illustrated in Fig. 1. The first set of samples was made as a 20  $\times$  20 array of solder bumps of eutectic Au-Sn solder (80Au-20Sn by weight, 71Au-29Sn by molar content) on Si substrates electroplated with 15–20  $\mu\text{m}$  Cu. The bumps were spherical caps 140–145  $\mu\text{m}$  in diameter and 55–65  $\mu\text{m}$  tall, and the array had a pitch of about 500  $\mu\text{m}$ . The bumps were made with the

(Received January 31, 2000; accepted April 18, 2000)

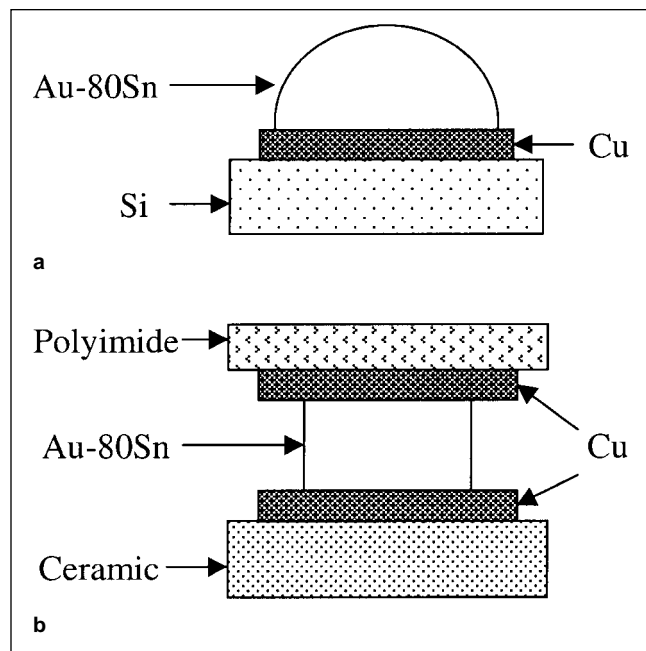


Fig. 1. Schematic diagrams of the sample geometries used in this study (a) solder bump: unjoined bump (b) solder joint: joined bump.

“bumped” variation of the Z-MAJIC™ process.<sup>4</sup> In this process a thermoplastic bonding sheet with a removable cover layer is tacked or laminated onto the substrate. The composite sheet has a pattern of cavities that expose the underlying Cu layer. Solder paste is deposited into the cavities and reflowed to form the bumps. The reflow treatment includes a 75 sec. expo-

sure above 280°C with a peak temperature of 315°C, slightly above the 280°C melting temperature of eutectic Au-Sn (Fig. 2a).<sup>5</sup> The cover layer is then removed, exposing the tops of the solder bumps for subsequent bonding.

The microstructure of the solder bumps was studied in three conditions: as-solidified, after up to eight “reflow” treatments to a peak temperature of 260°C, and after aging at 200°C for up to 120 days. (The “reflow” treatments do not actually melt the solder; the cycle is used to reflow Sn-3.5Ag joints that are used in the same devices in commercial practice.)

The second set of samples came from eutectic Au-Sn solder bumps, also made on Cu-plated ceramic substrate by the Z-MAJIC™ process, that were bonded to a layer of Cu-plated polyamide to complete the joint. In this case the joints were about 60 μm in diameter and 25 μm in height, while the Cu plated layers on the top and bottom pads were about 5 μm in thickness.

The microstructures of the solder joints were studied in three conditions: after aging at 150°C for 20 days, after aging at 200°C for up to 50 days, and after thermal cycling from -65°C to 150°C for 500 cycles. Metallographic studies were done on samples that were mounted in epoxy, then polished to observe and analyze the cross-sectional microstructure using an optical microscope and a scanning electron microscope (SEM) with a back-scattered electron (BSE) detector and an energy-dispersive x-ray (EDX) analyzer. It was found that some Cu was transferred from the Cu pad onto the solder surface during polishing.

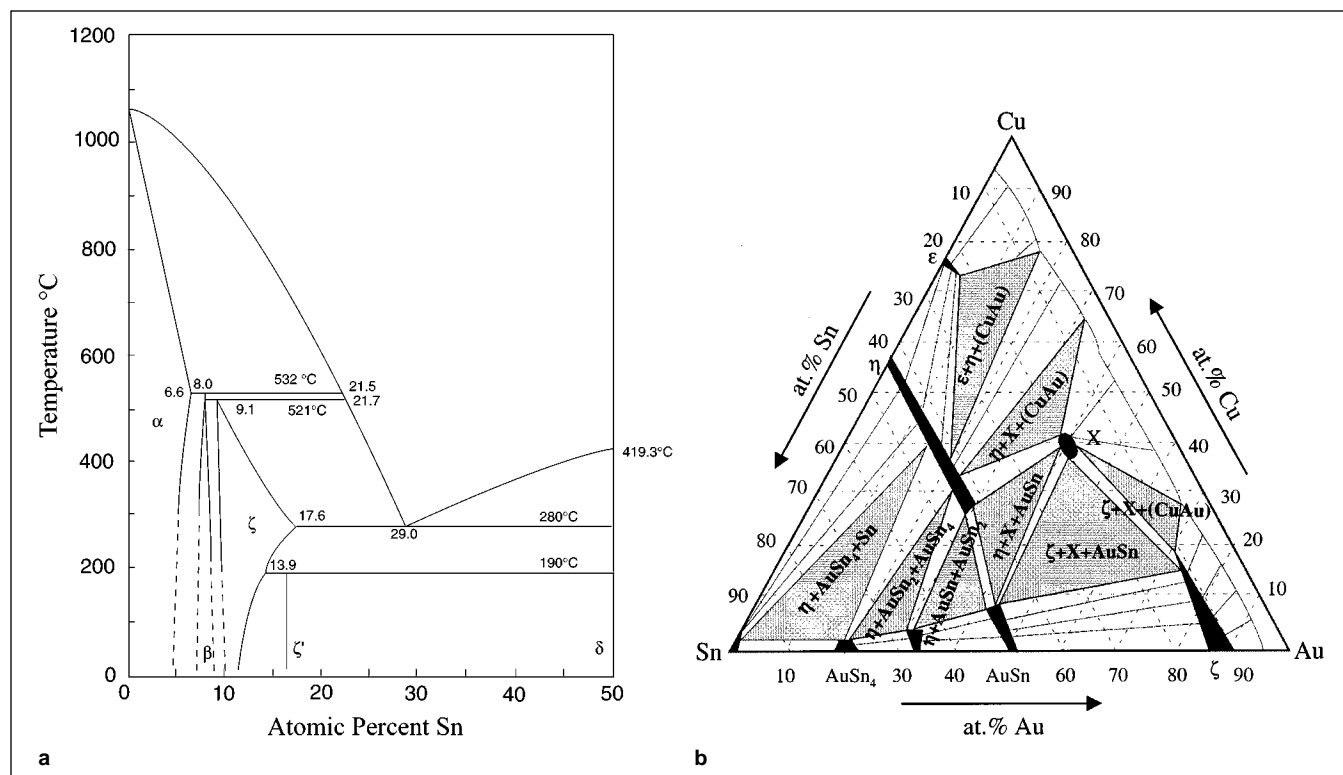


Fig. 2. (a) Au-AuSn binary phase diagram<sup>5</sup> (b) Isothermal cross section of the ternary CuAuSn system at 190°C<sup>6</sup>.

To remove this Cu, the samples were etched with dilute  $\text{HNO}_3$  before EDX analysis.

## RESULTS AND DISCUSSION

### Solder Bumps

The microstructures of all the solder bumps studied resemble that of the as-solidified bump shown in Fig. 3. As expected from the binary phase diagram (Fig. 2a), the bulk of the solder is a eutectic mixture of the  $\delta$ -phase (nominally AuSn) and  $\zeta$ -phase (a Au-rich intermetallic with a broad composition range, from about 9 to almost 18 atomic percent Sn). The Cu interface is coated with a thick, irregularly shaped intermetallic layer that is predominantly  $\zeta$ -phase with a significant addition of Cu substituting for Au. In addition, the aged samples have a double layer of Cu-rich intermetallic between the  $\zeta$ -phase and the Cu substrate; the inner layer is nominally  $\text{Cu}_3\text{Au}$ , the outer is nominally CuAu.

### As-soldered Bumps

The cross-sectional microstructure of the as-sol-

dered bump is shown in Fig. 3. The interior of the bump has a fine-scale eutectic microstructure. The bright constituent in the eutectic is  $\zeta$ -phase while the darker constituent is  $\delta$ -phase. Cu was detected throughout the bulk solder by EDX analysis, suggesting that Cu dissolved into the molten solder during reflow. The composition of the bulk eutectic is approximately 60Au-10Cu-30Sn (all compositions are in mole fraction unless stated otherwise). Since the nominal composition of eutectic Au-Sn is 71Au-29Sn, it appears that Cu substitutes for Au in the eutectic. However, due to the very fine spacing of the lamellae it was not possible to determine how Cu partitions between the two phases.

The mushroom-shaped interfacial intermetallic was identified by EDX analysis as a ternary CuAuSn that has a composition of (66–70)Au(16–20)Cu(13–15)Sn, with the Cu content increasing slightly toward the interface. If we assume that the Cu substitutes for Au, this phase is  $\zeta$ -phase in its ternary,  $(\text{AuCu})_{4-10}\text{Sn}$  form. This conclusion is consistent with the proposed ternary phase diagram shown in Fig. 2b,<sup>6</sup> which suggests that the  $\zeta$ -phase can incorporate up to about 20Cu.

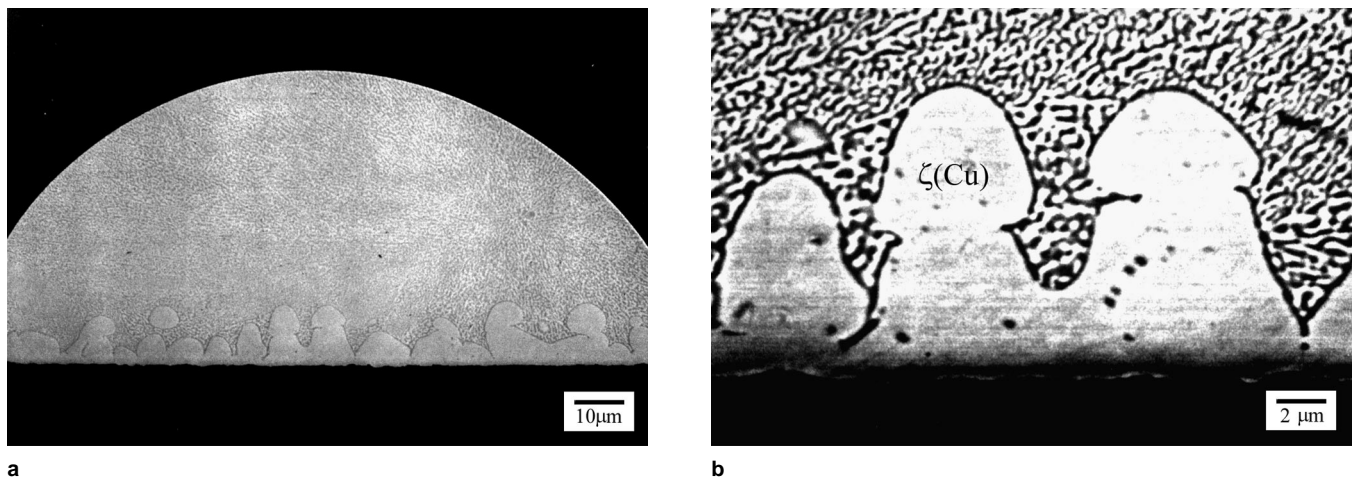


Fig. 3. Cross-sectional micrographs of as-soldered solder bump (a) SE image at low magnification (b) BSE image at high magnification.

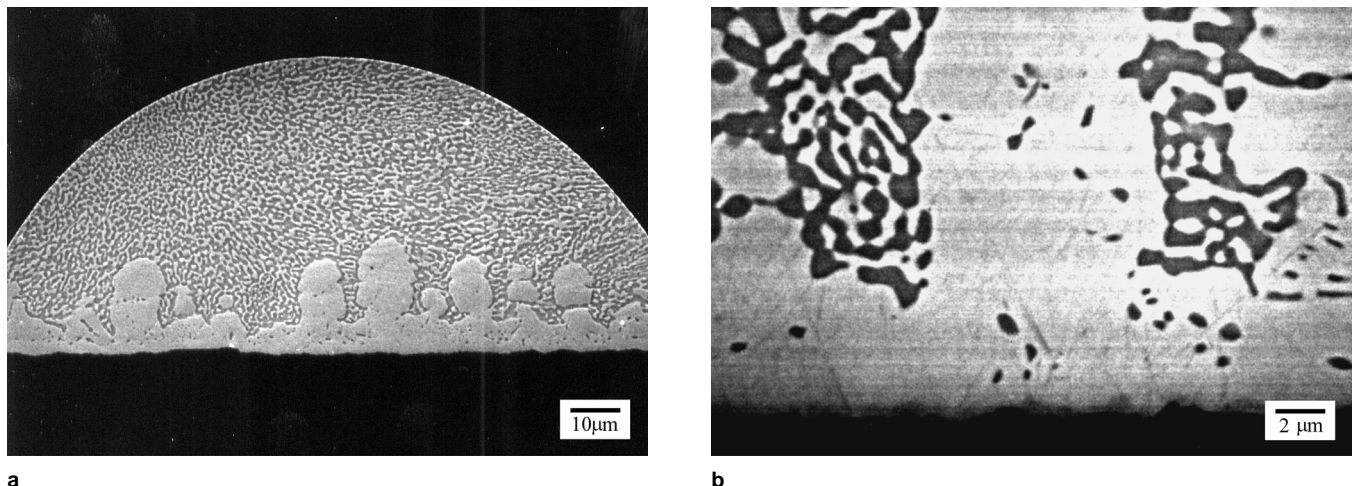


Fig. 4. Cross-sectional micrographs of 8 times-reflowed (260°C peak temperature) solder bump (a) SE image at low magnification (b) BSE image at high magnification.

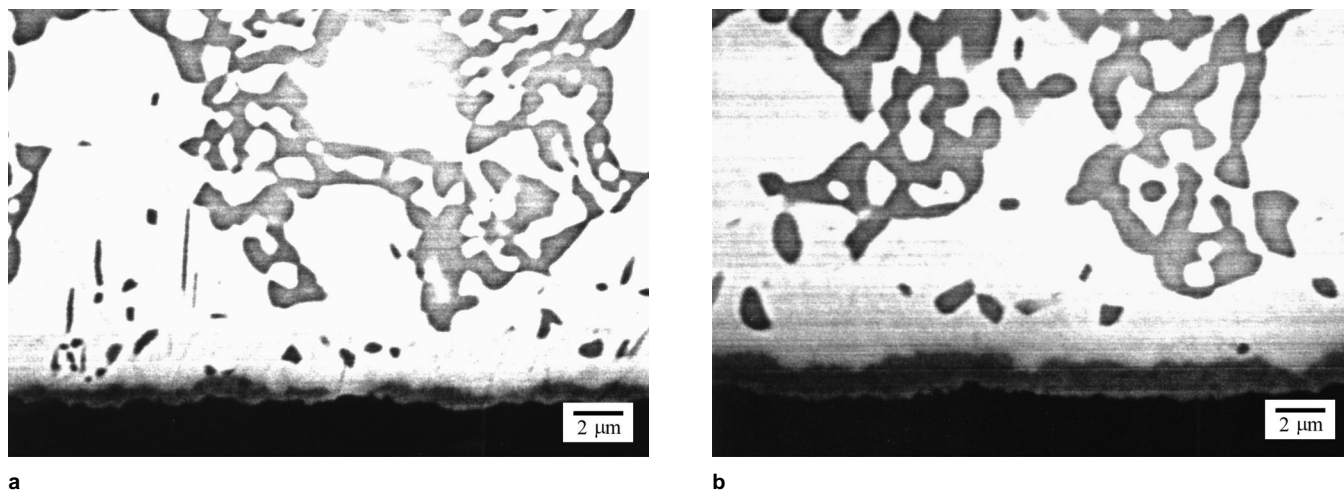


Fig. 5. Cross sectional BSE images of solder bumps aged at 200°C for (a) 1 day, and (b) 4 days.

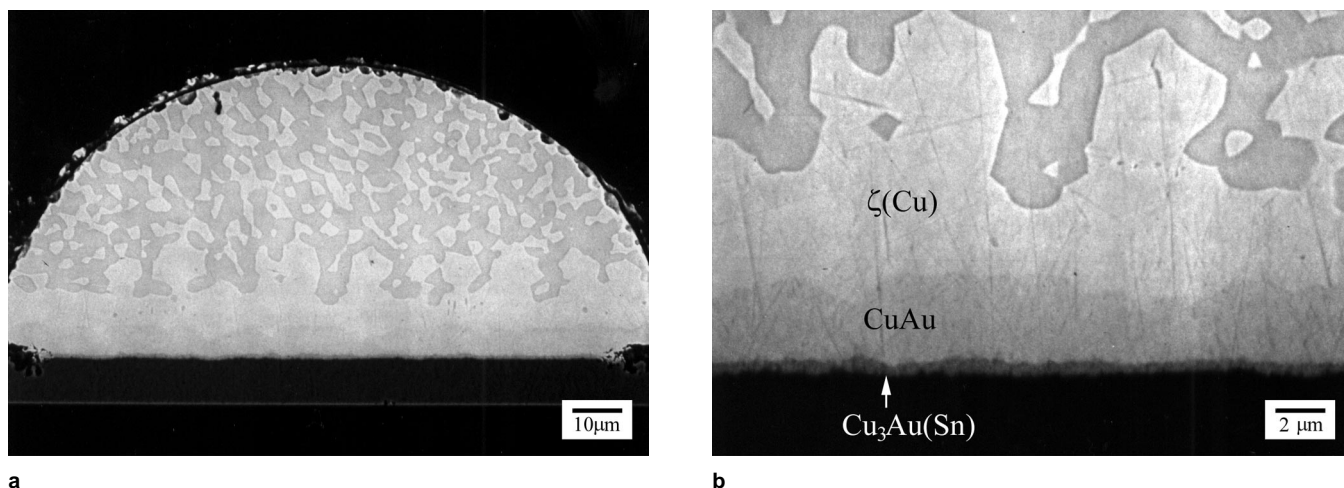


Fig. 6. Cross-sectional SEM micrographs of solder bump aged at 200°C for 80 days (a) at low magnification (b) at high magnification.

A close examination of BSE images shows that there is a thin layer of a third phase at the Cu- $\zeta$  interface. EDX analysis revealed that this phase is relatively rich in Cu, but, since the layer is no more than 0.5  $\mu\text{m}$  thick, its composition could not be measured precisely.

The overall microstructure of the bump is relatively easy to understand, based on a solid-liquid reaction between molten eutectic Au-Sn solder and the Cu substrate. When the solder is molten, between 280°C and 315°C, Cu dissolves and gradually accumulates in the liquid solder. Since the Cu acts basically like Au, we can infer from the binary phase diagram (Fig. 2a) that the Cu addition produces a hypoeutectic composition, from which a Cu-containing  $\zeta$ -phase precipitates along the Cu interface. Since Cu is believed to be the most mobile species in the Au-Cu-Sn system,<sup>7-9</sup> the rate of growth of this intermetallic is determined by the rate of Cu diffusion through it to the interface between the intermetallic and the residual molten solder. Since the temperature is only slightly above the eutectic temperature, the residual liquid retains a near-eutectic composition, and solidifies into the eutectic constituent on cooling.

#### “Reflowed” Bumps

Figure 4a shows the etched cross-section of a bump that was given eight “reflow” cycles with a peak temperature of 260°C. This treatment causes an obvious coarsening of the lamellae within the eutectic constituent, making them large enough for EDX analysis. The measured composition of the  $\zeta$ -phase is (73–76)Au(9–12)Cu(14–15)Sn, which is consistent with a straightforward substitution of Cu for Au. The measured composition of the  $\delta$ -phase was (46–47)Au(50–52)Sn with less than 2Cu. It appears that the Cu in the eutectic segregates almost completely to the  $\zeta$ -phase. This result disagrees slightly with the proposed ternary phases diagram (Fig. 2b),<sup>6</sup> which does show a preferential segregation to  $\zeta$ , but suggests a partition that leaves the  $\delta$ -phase with a significant Cu content.

The  $\zeta$ -phase layer at the interface grows very little, if at all, in these “reflows,” which do not actually melt the solder. However, its composition is enriched in Cu. EDX analysis of the  $\zeta$ -phase at the interface gives the composition (64–70)Au(16–25)Cu(12–15)Sn. Moreover, the layer has become decorated with a distribution of precipitates that were identified as  $\delta$ -phase

(AuSn). The 190°C isothermal section of the proposed phase diagram, Fig. 2b, suggests that the system enters a three-phase region,  $\zeta + \delta + \text{“X”}$ , when the Cu content of the  $\zeta$  increases above 20 atomic percent and the Sn content is greater than about 15%. We therefore expected to find precipitates of X-phase (40Au40Cu20Sn) within the  $\zeta$ -layer, but found none. It appears that the  $\zeta$ -phase is simply rich in Cu.

The intermetallic layer along the  $\zeta$ -Cu interface (Fig. 4b), also grows during this thermal cycle. Isolated regions of it were thick enough for EDX analysis, which gave its composition as (46–48)Cu(45–47)Au(7–8)Sn. The film is CuAu with a bit of entrapped Sn.

#### Aging at 200°C

When the solder bump is aged at 200°C, the eutectic Au-Sn lamellae coarsen and become globular, the  $\zeta$ -layer at the interface accumulates Cu, and Cu-rich intermetallics develop at the  $\zeta$ -Cu interface. Since Cu forms Cu-rich intermetallics with both Au and Sn, it is not surprising to find an additional intermetallic at the Cu interface.

The early-stage evolution of the microstructure is illustrated in Fig. 5, which includes BSE images of bumps aged at 200°C for 1 day and 4 days. The  $\zeta$ -phase layer at the interface does not appear to grow, but the  $\delta$ -phase precipitates that are within it grow and become more distinct. The CuAu layer at the Cu interface grows noticeably. EDX analysis suggests that this compound is slightly Cu-rich, with a composition near 55Cu45Au, and gradually loses Sn, going from 1–2Sn after 1 day to below 1 Sn after 2 days.

Figure 6 shows the microstructure after 80 days at 200°C. The eutectic has now become quite coarse, and the interfacial  $\zeta$ -layer has gradually thickened, primarily by filling in the troughs between the mushroom-shaped protrusions. The CuAu layer has thickened at nearly constant composition. A third intermetallic layer has appeared on the Cu side. This layer, which is not clearly seen until after about 50 days aging, has a composition (78–80)Cu(17–20)Au(1–2)Sn, showing that it is  $\text{Cu}_3\text{Au}$  with a possible enrichment of Cu and a small addition of Sn. Since the CuAu and  $\text{Cu}_3\text{Au}$  layers are formed by solid-solid reaction between the  $\zeta$  layer and the Cu substrate and since the Sn source is the  $\zeta$  layer, it is interesting that a small amount of Sn was entrapped in the  $\text{Cu}_3\text{Sn}$  layer on the Cu side, even though the CuAu layer was nearly free from Sn. Considering the gradual loss of Sn from the initial CuAu layer during aging and assuming the Sn solubility in CuAu at 200°C is small, Sn may move out from the CuAu layer and be entrapped in the  $\text{Cu}_3\text{Au}$  layer.

The Cu content of the phases within the eutectic has also increased. The  $\zeta$ -phase composition is (61–63)Au(25–29)Cu(10–12)Sn, and the  $\delta$ -phase (AuSn) now contains measurable Cu (about 7Cu). No X-phase is found.

On further aging the eutectic continues to coarsen, the interfacial  $\zeta$ -phase layer gradually becomes more enriched in Cu, without significant thickening or X-

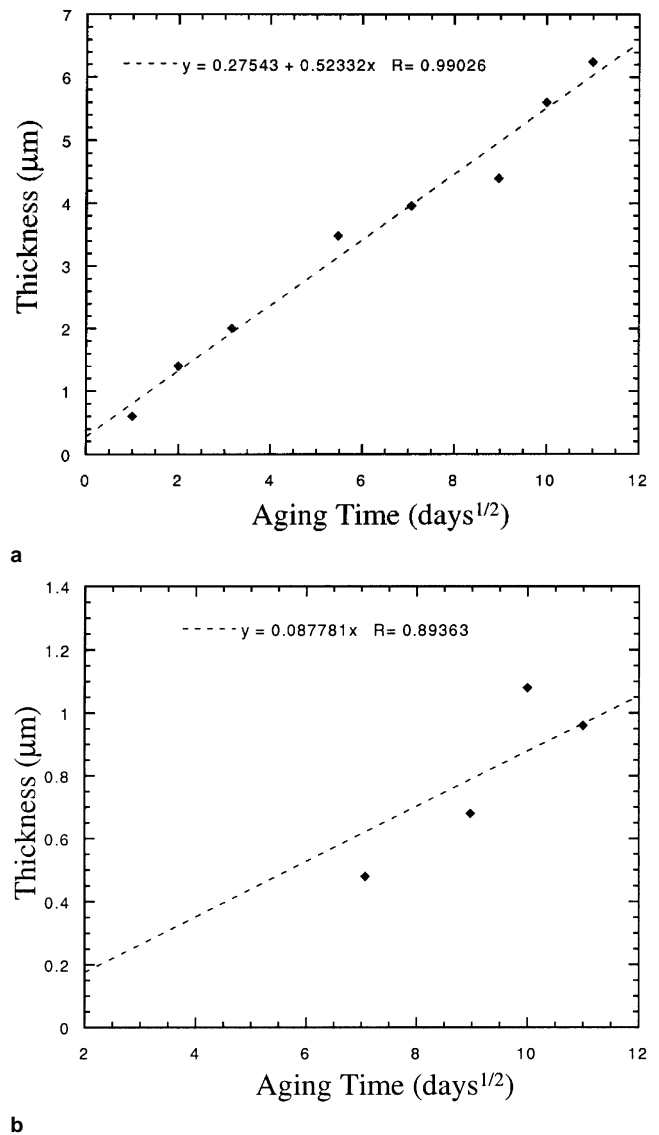


Fig. 7. Thickness of (a) the CuAu layer, and (b) the  $\text{Cu}_3\text{Au}$  layer in solder bumps with the square root of aging time at 200°C.

phase precipitation, and the CuAu and  $\text{Cu}_3\text{Au}$  intermetallic layers grow at essentially constant composition.

The growth of the CuAu and  $\text{Cu}_3\text{Au}$  layers is plotted in Fig. 7. While the data is limited, both layers seem to show normal diffusion-controlled growth kinetics and thicken as  $t^{1/2}$ . The development of the compound intermetallic layer hence resembles that of the Cu-Sn case analyzed by Mei, Sunwoo, and Morris;<sup>9</sup> the intermetallic grows by consuming the underlying Cu and the overlying layer of  $\zeta$ -phase. Once both intermetallic layers have formed, they maintain a constant thickness ratio during growth. Since the CuAu layer is initially thicker, it also thickens more rapidly.

## Solder Joints

### As-soldered Joints

The solder joints studied here differ from the solder bumps in that they are smaller (60  $\mu\text{m}$  diameter, 25  $\mu\text{m}$  height vs. 140  $\mu\text{m}$  diameter, 60  $\mu\text{m}$  height), they

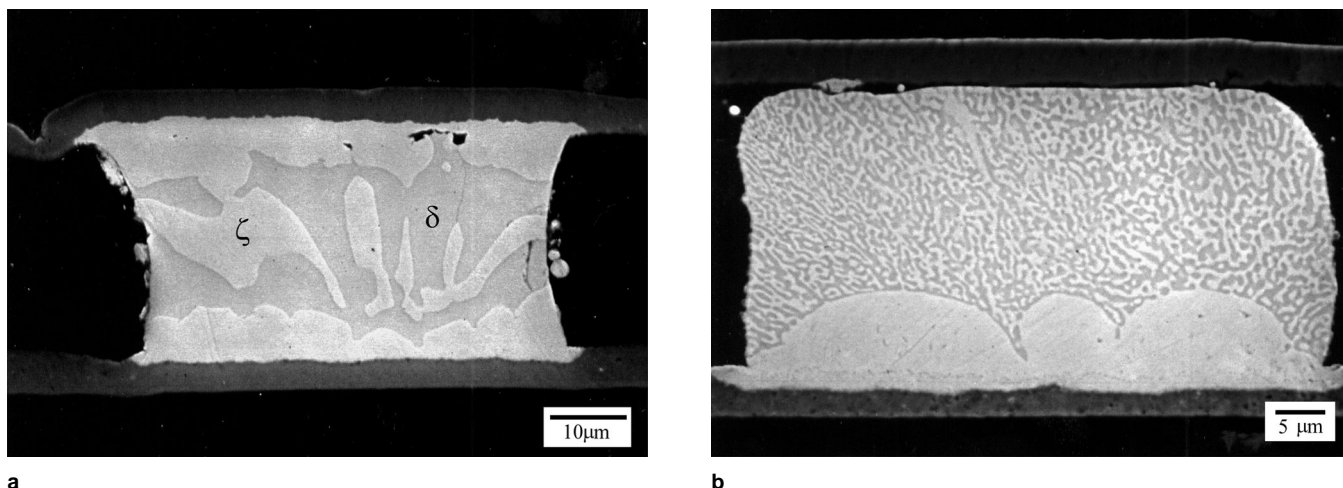


Fig. 8. Cross-sectional SEM micrographs of as-soldered joints with (a) typical microstructure, and (b) less common microstructure.

contact Cu on both sides, and they have undergone a second lamination reflow (10 min above 280°C, peak at 310°C) in forming the joint. Moreover, while we do not know the precise thermal profile during joint solidification, the fact that the joints are enclosed between the bonded layers suggests that the cooling rate after final lamination reflow is significantly slower than that of the exposed solder bumps described above.

The consequence of these changes is to produce a joint microstructure that is dramatically different from that of the solder bumps. The substantial majority of the joints examined have the microstructure illustrated in Fig. 8a, with thick intermetallic coatings at both interfaces and a coarse, two-phase structure in the center of the joint. The two phases in the center of the joint are δ-phase, which appears dark in the SEM micrograph, and ζ-phase, which is relatively light. The δ-phase is almost stoichiometric AuSn with very little Cu. The ζ-phase has the measured composition (65–68)Au(19–22)Cu(13–14)Sn. The thick intermetallic layers at the interfaces are nominally ζ-phase. However, they are highly enriched in Cu, with composition (57–59)Au(29–31)Cu(10–12)Sn. This composition is outside the ζ-field of the proposed phase diagram (Fig. 2b), which suggests that the intermetallic contains precipitates. While these are difficult to resolve in the SEM, they become evident on aging, as discussed below. A single Cu-rich intermetallic layer can also be resolved at the Cu interface. Its nominal composition is (56–59)Cu(36–39)Au(4–6)Sn, which appears to be a Cu-rich CuAu with some entrapped Sn.

In Fig. 9, a schematic vertical section along 71Au29Sn-Cu is shown. This diagram was constructed to examine the as-soldered joint microstructure based on the Karlsen et al.'s isothermal sections near 320°C,<sup>10</sup> which is close to the peak temperature of the present study. According to Karlsen et al., phase A is a high temperature phase which has a nominal composition of (42–47)Au(33–37)Cu20Sn. This phase transforms into the lower temperature phase X shown in Fig. 2b.

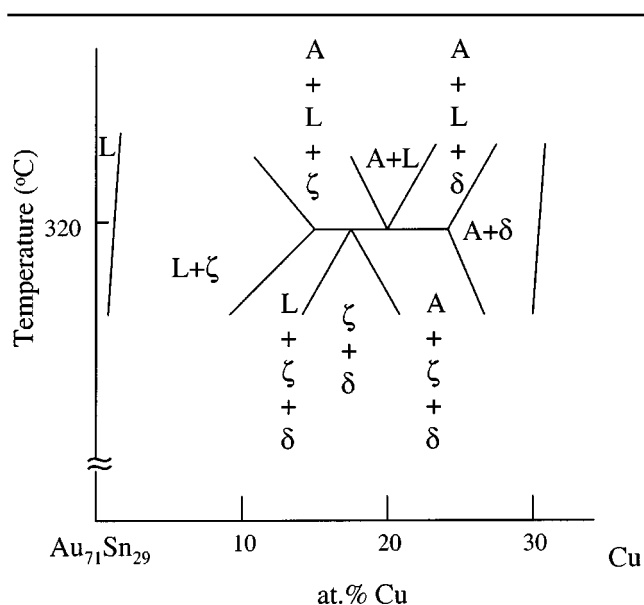


Fig. 9. Schematic vertical section along 71Au29Sn-Cu.

Since the joints have a much larger surface to volume ratio than the bumps examined earlier and because they were held above 280°C for much longer, more Cu can dissolve into the molten solder, and the melt composition can reach the ζ + δ region. Since we could not find A phase in the as-soldered sample, the Cu composition during reflow is most likely in the ζ + δ region. It follows that the joint solidifies completely during reflow; hence no liquid remains to form eutectic on subsequent cooling, and no lamellar structure is formed. This analysis suggests that the major factor controlling the joint microstructure is the amount of Cu dissolution during the reflow process, which is controlled by the reflow profile and the sample geometry. If the Cu dissolution is sufficient to place the bulk composition within the ζ + δ two-phase region the joint solidifies into a coarse microstructure. Otherwise, liquid remains at the end of the reflow and solidifies into a lamellar eutectic. We have occasion-

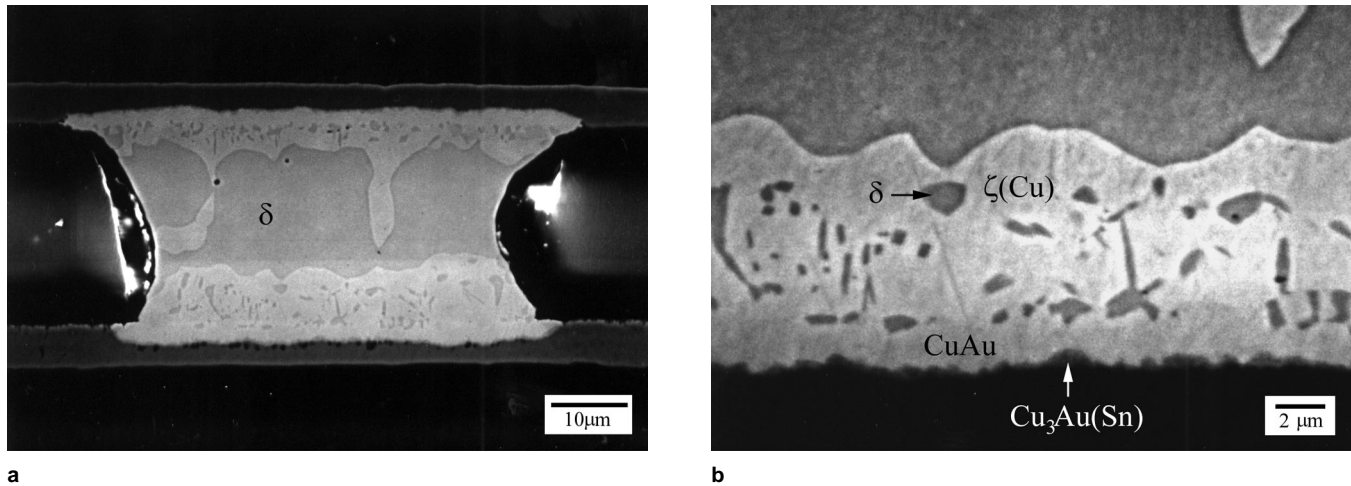


Fig. 10. Cross-sectional SEM micrographs of solder joint aged at 200°C for 10 days (a) at low magnification (b) at high magnification.

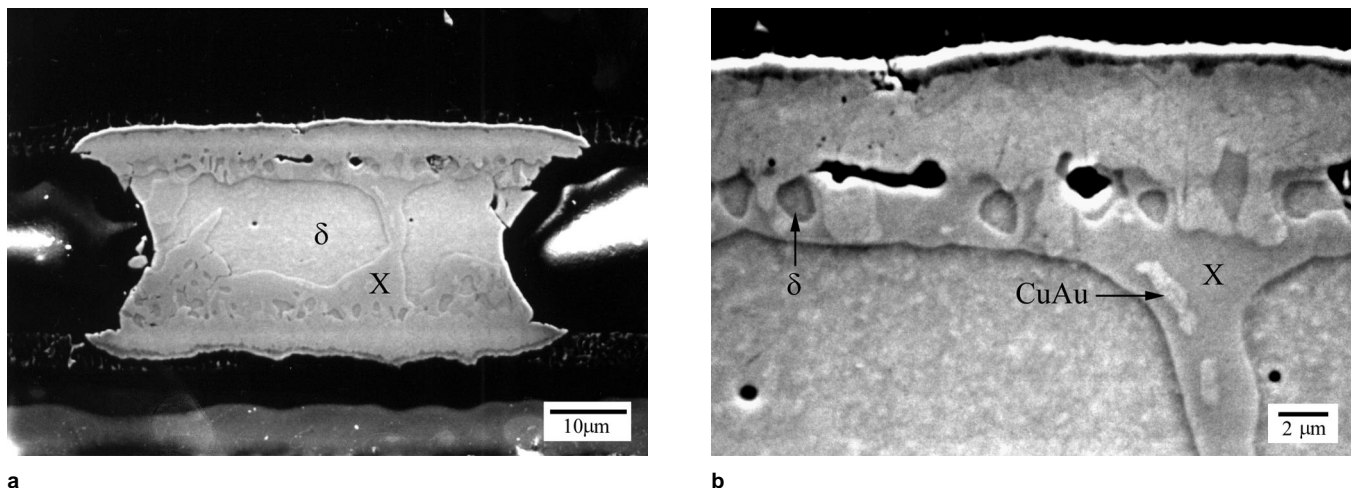


Fig. 11. Cross-sectional SEM micrographs of solder joint aged at 200°C for 50 days (a) at low magnification (b) at high magnification.

ally found joints that have a fine eutectic microstructure in the interior. An example is shown in Fig. 8b. This microstructure appears to have two different causes. In some of these joints the upper Cu pad was incompletely bonded, which would cause insufficient Cu dissolution and eutectic solidification. In other joints we suspect that the local temperature during reflow was low, resulting in reduced diffusion of Cu

#### Aging at 200°C

Aging at 200°C results in a steady accumulation of Cu within the joint, causing the monotonic growth of the Cu-rich intermetallics, which eventually bridge the joint.

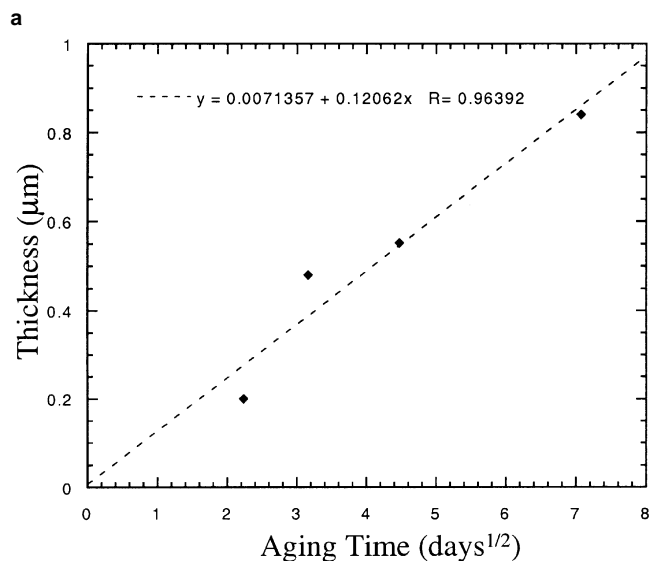
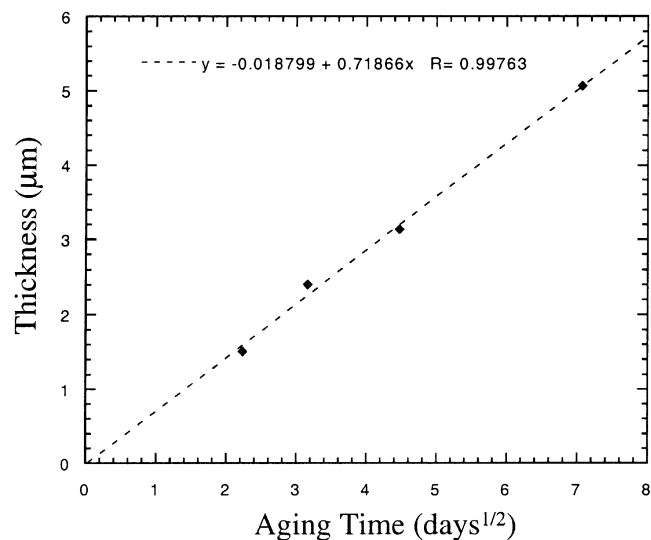
Figure 10 illustrates the microstructure after 10 days aging at 200°C. The  $\zeta$ -phase layers at the interfaces have thickened, and become significantly richer in Cu. The  $\zeta$ -phase in the layer has the composition (58–61)Au(28–31)Cu(10–11)Sn. The  $\zeta$ -phase is decorated with precipitates that prove to be  $\delta$ -phase (AuSn), as in the solder bumps described above. While the  $\zeta$ -phase is supersaturated with respect to precipitation of X-phase (at least, according to the phase diagram in Fig. 2b), no X-phase precipitates appear. Cu-rich inter-

metallic layers have formed at the Cu interface, as in the solder bumps. The outer layer is nominally CuAu, with almost no detectable Sn, and the inner layer is nominally  $\text{Cu}_3\text{Au}$  with about 2Sn included.

The microstructure and intermetallic composition are roughly similar for samples aged for 20 days, though with a further increase in Cu content.

Aging for 50 days, however, produces a dramatic change in the phase distribution within the joint. The microstructure is illustrated in Fig. 11. The thick intermetallic layers have bridged the joint. They are different in appearance and have also, apparently, changed in phase. EDX analysis gives the composition (40–41)Au(41–42)Cu(17–19)Sn, which is very close to the reported composition of the X-phase ternary intermetallic (40Au40Cu20Sn).

As shown in Fig. 11b, the X-phase is decorated with small precipitates. EDX analysis shows that the larger and darker of these are  $\delta$ -phase (AuSn). The smaller, lighter precipitates prove to be CuAu. No  $\zeta$ -phase was found. These results are puzzling, since there is no  $\delta + X + \text{CuAu}$  region in the proposed phase diagram, and the X-phase can only be accessed by passing through compositions where X and  $\zeta$  coexist. It ap-



**b**  
Fig. 12. Thickness of (a) the CuAu layer, and (b) the Cu<sub>3</sub>Au layer in solder joints with the square root of aging time at 200°C.

pears that there may be a three phase region of  $\zeta + \delta + \text{CuAu}$  which moves into  $\delta + \text{X} + \text{CuAu}$  region with increasing Cu content. Experiments for verification of its details are in progress.

The Cu-rich intermetallic layers at the interface have also coarsened. The CuAu layer appears to be slightly Cu-rich, with composition (53–54)Cu(46–47)Au(<1)Sn. The Cu<sub>3</sub>Au layer is also slightly Cu-rich, with composition (76–79)Cu(19–22)Au<sub>2</sub>Sn. The growths of the two intermetallic layers are plotted as a function of time in Fig. 12. As in the case of the solder bumps, their thicknesses increase as  $t^{1/2}$ . However, the growth rates are somewhat higher in the joints than in the bumps, which is consistent with the generally higher Cu content of the  $\zeta$ -phase layer.

#### Aging at 150°C and Thermal Cycling to 150°C

For comparison joint samples were studied after two alternative treatments: isothermal aging for 20

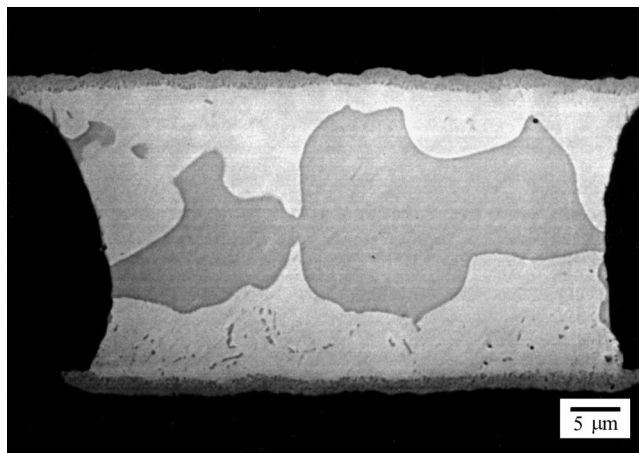


Fig. 13. Cross-sectional BSE image of solder joint aged at 150°C for 20 days.

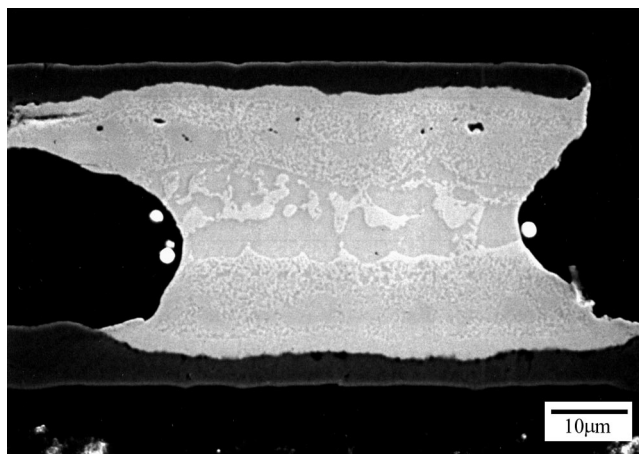


Fig. 14. Cross-sectional SEM micrograph of solder joint thermally cycled from –65 to 150°C for 500 cycles.

days at 150°C and thermal cycling from –65°C to 150°C for 500 cycles.

Figure 13 shows a cross-section of the sample that was isothermally aged for 20 days at 150°C. Thick  $\zeta$ -phase intermetallics coat the interfaces, and have almost bridged the joint. Their composition is (60–64)Au(23–27)Cu(12–14)Sn, which is close to that after 10 days aging at 200°C. The layer is decorated with a distribution of fine AuSn ( $\delta$ ) precipitates. Only one Cu-rich intermetallic is found at the Cu interface. Its composition is (53–54)Cu(41–42)Au(5–6)Sn, which is very close to composition measured in the as-solidified joint.

Figure 14 shows the complex microstructure of a joint that was cycled 500 times from –65°C to 150°C, beginning from the as-solidified condition. The overall deformation of the joint is evident. Also, a short crack has developed at the upper right-hand edge of the joint near the Cu interface. This crack appears to follow the CuAu- $\zeta$  interface, and does not appear to be affected by the process voids (from flux or out-gassing from the substrate) that are located slightly farther beneath the interface.

The  $\zeta$ -phase layer in this cycled joint is multi-phase



and is broken up into small volumes less than 1  $\mu\text{m}$  in diameter. Its overall composition is (46–56)Au(30–36)Cu(14–18)Sn, which would appear to place it within the three-phase  $\zeta + X + \text{CuAu}$  field in the proposed phase diagram. The high Cu content suggests that the mechanical work associated with the thermal cycle enhances the diffusivity of Cu. The fine-grained structure that is present in the sample pictured here would certainly favor a high diffusivity via grain boundary diffusion.

### SUMMARY AND CONCLUSIONS

As-soldered eutectic Au-Sn microbumps on Cu have a thick  $\zeta$ -phase intermetallic along the Cu interface with periodic mushroom-shaped protrusions, and a fine eutectic lamellar structure through the bulk. Both isothermal aging at 200°C and thermal cycling treatments coarsen the eutectic and significantly increase the Cu content of the intermetallic, which develops a distribution of  $\delta$ -phase (AuSn) precipitates. Despite the high Cu content of the  $\zeta$ -phase ( $> 25\text{Cu}$ ), however, no X-phase (40Au40Cu20Sn) is found. Prolonged aging at 200°C leads to the formation of a double layer of Cu-rich intermetallics along the Cu interface. The intermetallics are, nominally,  $\text{Cu}_3\text{Au}$  on the Cu-side and CuAu on the  $\zeta$ -phase side. Both intermetallics thicken with  $t^{1/2}$ .

Eutectic microjoints, 60  $\mu\text{m}$  in diameter by 25  $\mu\text{m}$  height, were formed between Cu pads on Si and polyimide. The typical microstructure in the as-soldered condition has thick, Cu-rich  $\zeta$ -phase intermetallics along the interfaces, with only a few large grains in the interior. As the joints are aged at 200°C, the  $\zeta$ -phase becomes enriched in Cu, taking in as much as 35Cu. It is decorated by  $\delta$ -phase (AuSn). However, no X-phase is found until 50 days aging. Between 20 and 50 days aging at 200°C, the  $\zeta$ -phase fully transforms to X-phase with a very nearly stoichiometric composition (40Au40Cu20Sn). The X-phase contains precipitates of both  $\delta$ -phase (AuSn) and CuAu, but no residual  $\zeta$ -phase was found. Thermal cycling from 65°C to 150°C caused the  $\zeta$ -phase interfacial layer to decompose into a very fine-grained distribution of two or more phases. Like the microbumps, the microjoints also formed a double-layer film of  $\text{Cu}_3\text{Au}$  and CuAu along the Cu interface. The Cu-rich intermetallics thickened with  $t^{1/2}$  while preserving a constant thickness ratio.

Our principle conclusions are that: (1) As-soldered microjoints of eutectic AuSn on Cu can have microstructures that are very coarse on the scale of the joint, where the microstructure is dependent on the amount of Cu dissolution during reflow process. These joints contain so few grains that one should be cautious when using macroscopic property data to predict their behavior. (2) Thick interfacial intermetallics form during soldering. These are primarily  $\zeta$ -phase ( $\text{Au}_{4-10}\text{Sn}$ ), and their evolution is not well predicted by the ternary phase diagram that has recently been proposed for the Au-Cu-Sn system.<sup>6</sup> (3) In particular, after accumulating a significant Cu content, the  $\zeta$ -phase intermetallic may convert into an "X"-phase whose properties are not well known. (4) The interfacial intermetallic can be decomposed into a fine-grained mixture of two or more phases by thermal cycling. (5) The phase relationships in the aged, Cu-rich joints differ from those in the ternary Au-Cu-Sn phase diagram proposed by Zakel and Reichl,<sup>6</sup> particularly in the vicinity of the "X"-phase field. Phase evolution in this ternary system will be further studied.

### ACKNOWLEDGEMENTS

This research was supported by Fujitsu Computer Packaging Technologies and by the Director, Office of Energy Research, Office of Basic Sciences, U.S. Department of Energy, under Contract No. DE-AC03-76SF00098.

### REFERENCES

1. J.W. Morris, Jr., *J. Korean Phys. Soc.* 35, 335 (1999).
2. K.N. Tu and R. Rosenberg, *Jpn. J. Appl. Phys., Suppl. 2* Part 1, 633 (1974).
3. J.S. Hwang, *Modern Solder Technology for Competitive Electronics Manufacturing* (New York: McGraw-Hill Co., 1996), p. 418.
4. M.T. McCormack, H. Jiang, S.I. Beilin, B. Chou, and M. Peters, *EEP-Vol.26-2, Adv. Electron. Pkg.* 2, 1807 (1999).
5. G.S. Matijasevic, C.C. Lee, and C.Y. Wang, *Thin Solid Films* 223, 276 (1993).
6. E. Zakel and H. Reichl, *Flip Chip Technologies*, ed. J.H. Lau (New York: McGraw-Hill Co., 1996), p. 451.
7. S. Nakahara, R.J. McCoy, L. Buene, and J.M. Vandenberg, *Thin Solid Films* 84, 185 (1981).
8. M.R. Pinnel and J.E. Bennett, *Metall. Trans.* 3, 1989 (1972).
9. Z. Mei, A.J. Sunwoo, and J.W. Morris, Jr., *Metall. Trans. A* 23A, 857 (1992).
10. O.B. Karlsen, A. Kjekshus, and E. Rost, *Acta Chem. Scan.* 46, 147 (1992).